

Minimization of torque ripple in switched reluctance motor drives using direct instantaneous torque control

J. Castro, P. Andrada and B. Blanqué

Electronically Commutated Drives Group (**GAECE**), Departament d'Enginyeria Elèctrica (**DEE**),
Escola Politècnica Superior d'Enginyeria de Vilanova i la Geltrú (**EPSEVVG**).
Universitat Politècnica de Catalunya (**UPC**), **BARCELONATECH**
Avinguda Victor Balaguer 1, 08800 Vilanova i la Geltrú, Barcelona, Spain.
pere.andrada@upc.edu

Abstract. Torque ripple is an inherent characteristic of switched reluctance motor drives due to its double salient geometry and it is a serious drawback in applications that require smooth torque and high dynamic performances. This paper presents some contributions to the minimization of torque ripple in SRM using direct instantaneous torque control (DITC). Direct torque controller is simulated using Matlab/Simulink and then implemented in a DSPACE ACE kit 1006 CLP that includes a processor board with an AMD Opteron™ running at 2.6 GHz. Finally, experimental results are shown and they are compared with those obtained using conventional angle control.

Key words

Switched reluctance motor, torque ripple, direct torque control

1. Introduction

The switched reluctance motor (SRM) is gaining recognition in the electric drive market due to its simple and rugged construction, low expected manufacturing cost, fault tolerance capability, high efficiency and high torque to inertia ratio. Despite these advantages, the SRM has some disadvantages: it requires an electronic control and shaft position sensor, a huge capacitor is needed in the DC link and the double salient structure causes noise and torque ripple. Torque ripple is a serious drawback of SRM in applications that require smooth torque and high dynamic performances. Up to now, some mechanical design solutions have been proposed for minimizing torque ripple although they usually reduce the maximum torque and have a limited range of operation. Torque ripple can be minimized over a wider operating range by using electronic torque control techniques. These techniques can be classified in [1-6]:

Indirect (controlled variable current or flux linkage)

- Current profiling with off-line calculation of profiles
- Current profiling with on-line calculation of profiles

- Flux linkage profiling with off-line calculation of profiles
- Harmonic injection

Direct (controlled variable instantaneous torque)

- Instantaneous torque control

This paper presents some contributions to the minimization of torque ripple in SRM using direct instantaneous torque control (DITC). The rest of paper is organized as follows: section 2 describes the proposed direct torque control of SRM, section 3 presents the simulation model in Matlab/Simulink, section 4 shows the experimental results and compares them with those obtained using a conventional angle control, and finally section 5 presents the conclusions drawn from this research.

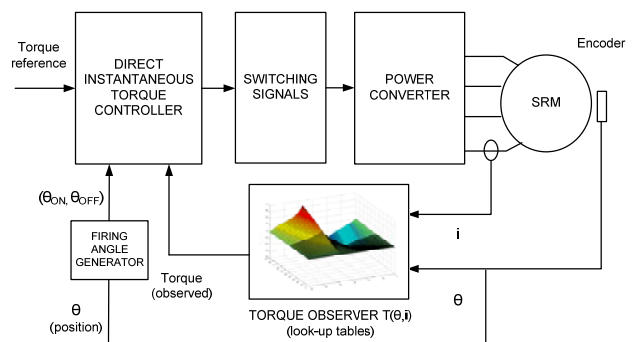


Fig. 1. Block diagram of the proposed DITC of the SRM

2. Description of the proposed DITC of SRM

The proposed block diagram of DITC of SRM is shown in Fig. 1. The instantaneous torque value is estimated from terminal variables (current and position) by means a look up table $T(\theta, i)$ that has been previously computed using FLUX, a finite element analysis software [7-8]. The torque-current-position profile obtained by finite element

Table I. Switching table

SWITCHING SIGNALS				PHASE STATES			
Phase n	Phase n+1	Phase n+2	Phase n+3	Phase n	Phase n+1	Phase n+2	Phase n+3
OFF	OFF	OFF	OFF	off	off	off	off
ON	OFF	OFF	OFF	Vcc/fw	off	off	-Vcc/off
ON	ON	OFF	OFF	Vcc/fw/-Vcc	Vcc/fw	off	off
OFF	ON	OFF	OFF	-Vcc/off	Vcc/fw	off	off
OFF	ON	ON	OFF	off	Vcc/fw/-Vcc	Vcc/fw	off
OFF	OFF	ON	OFF	off	-Vcc/off	Vcc/fw	off
OFF	OFF	ON	ON	off	off	Vcc/fw/-Vcc	Vcc/fw
OFF	OFF	OFF	ON	off	off	-Vcc/off	Vcc/fw
ON	OFF	OFF	ON	Vcc/fw	off	off	Vcc/fw/-Vcc

analysis for the four phases SRM prototype whose main data are listed in the appendix is given in Fig. 2.

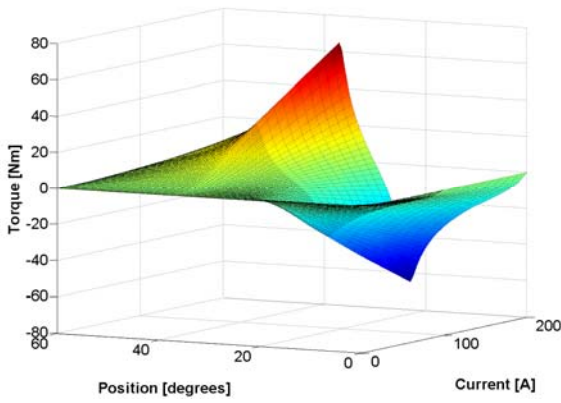


Fig 2. Torque-current-position profile of the SRM prototype

Then, the estimated value is compared with the reference torque, for determined firing angles (θ_{ON} , θ_{OFF}), in a direct instantaneous torque controller that generates the appropriate switching signals of the power converter. The power converter, in this case a four phases asymmetric converter with two power switches and two diodes per phase, has three states, which are denominated magnetization state (Vcc), freewheeling state (fw) and demagnetization state (-Vcc).

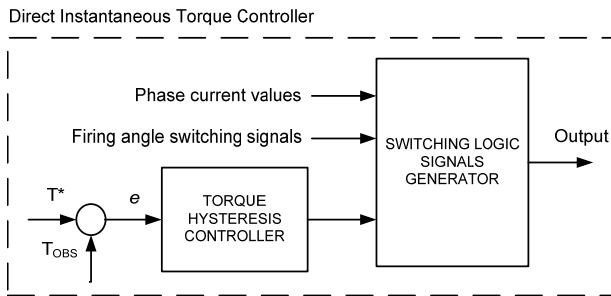


Fig. 3. Block diagram of DIT controller (per phase)

To minimize the torque ripple and maintain its value within a desired range, a controlled phase conduction overlap is performed. This overlap causes the definition of

three different conduction zones: ZONE 1 when the outgoing phase is on demagnetization state (-Vcc), ZONE 2 where there is only one phase in conduction and providing the total torque to the SRM (+Vcc/fw), and ZONE 3 where two adjacent phases are in conduction. In ZONE 3 the incoming phase (n+1) is the main torque producer (+Vcc), and the outgoing phase (n) is adding or subtracting the necessary torque to maintain the desired torque value (+Vcc/fw/-Vcc) before entering into the ZONE 1 and beginning the demagnetization of the phase. Table I shows the switching signals and the sequence of phase states at the different zones, according to the phase conduction period given by the generator of firing angles ($\theta_{ON}, \theta_{OFF}$).

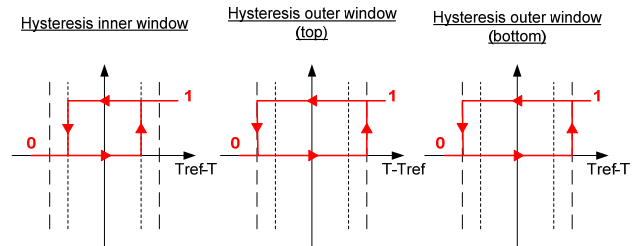


Fig. 4. Diagram of the hysteresis controllers

The rotor position (θ) and the generator of firing angles only indicate the conduction zone, but the actions that had to be performed to control the torque ripple are given by the blocks: torque hysteresis controller and generator of switching logic signals (see Fig. 3). The torque hysteresis controller produces the torque demand signals by comparing the observed and the reference torque using hysteresis regulators, set at different error values (also called windows). In one of these regulators the permitted error is set at values closer than the torque reference (inner window) and is only used when the conducting phase is in ZONE 2, and in other two regulators the error is set at values larger than the torque reference (outer window top and bottom) and are only used in ZONE 3. The outer window produces higher torque ripple but allows the outgoing phase demagnetization finish before entering the negative torque production region. Fig. 4 shows these torque hysteresis regulators. On the other hand, the generator of switching logic signals combines the firing angles, the

torque hysteresis regulator signals and the phase current value to produce the appropriate control signals to the power converter switches. This block is the intelligent core of DITC, which performs the logical combination of phase states and torque demand considering, also, the restriction of the maximum phase current.

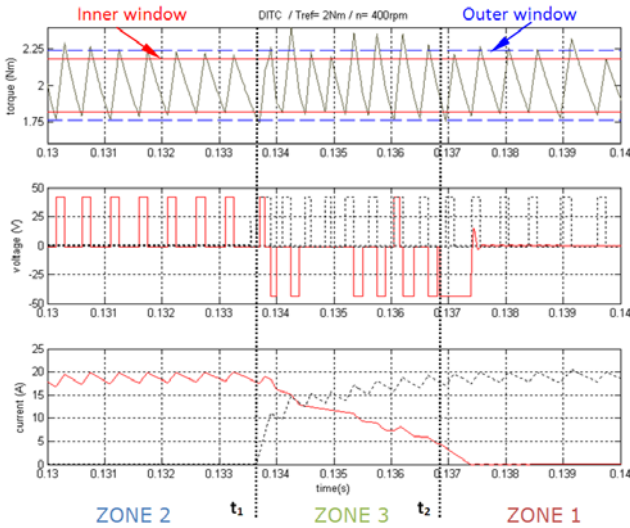


Fig. 5 Waveforms of instantaneous torque, voltage and current in which the different zones considered in the commutation process and the two hysteresis bands have been represented

Fig. 5 demonstrates the DITC working principle. The active phase (continuous line) stays in ZONE 2 up to the instant t_1 , when begins the phase overlap and it becomes the outgoing phase. In this period, the active phase is the only torque producer and its values are contained within the outer window, because is the inner window torque hysteresis regulator the producer of the torque demand signals. From the instant t_1 up to t_2 (ZONE 3), the incoming phase (dotted line) becomes the main torque producer and the outgoing phase has an auxiliary role adding or subtracting the necessary torque to maintain the torque value within a desired range. When the torque value exceed the outer window the outgoing phase reduces the total torque value producing negative torque (-Vcc), also producing positive torque (+Vcc) when the incoming phase is not able to produce enough torque and total torque value falls over the outer band. Finally, at the instant t_2 , the end of conduction period of the outgoing phase is reached entering in ZONE 1 when phase is demagnetized. The cycle continues with the active phase (dotted line) and the next phase.

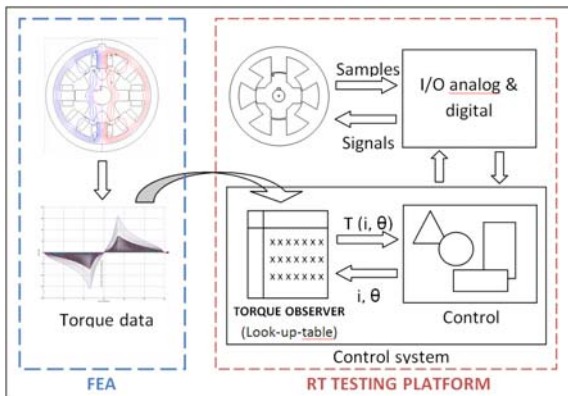


Fig. 6. Torque observer integration into the RT control system

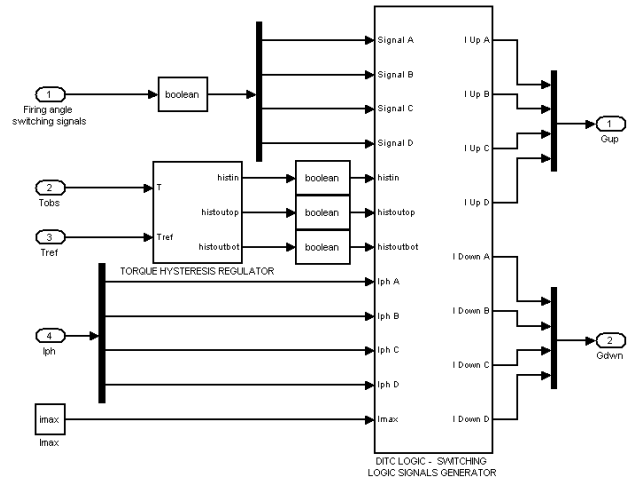


Fig. 7. Simulink block diagram of the DIT controller

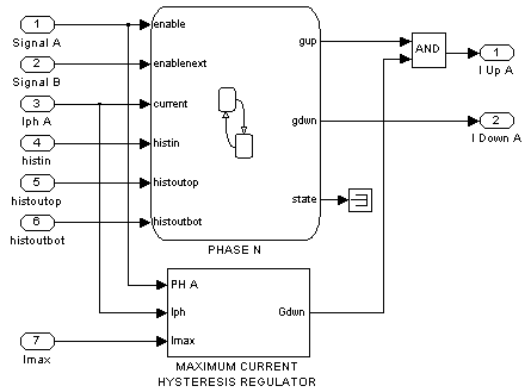


Fig. 8. Block diagram of the generator of switching logic signals (per phase)

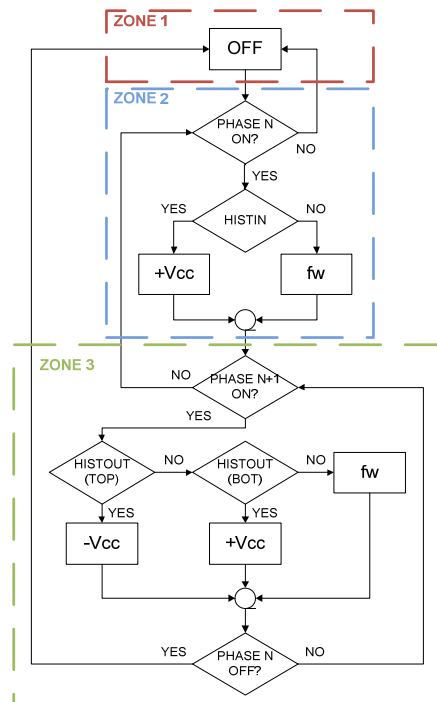


Fig. 9. Mealy finite-state machine flowchart

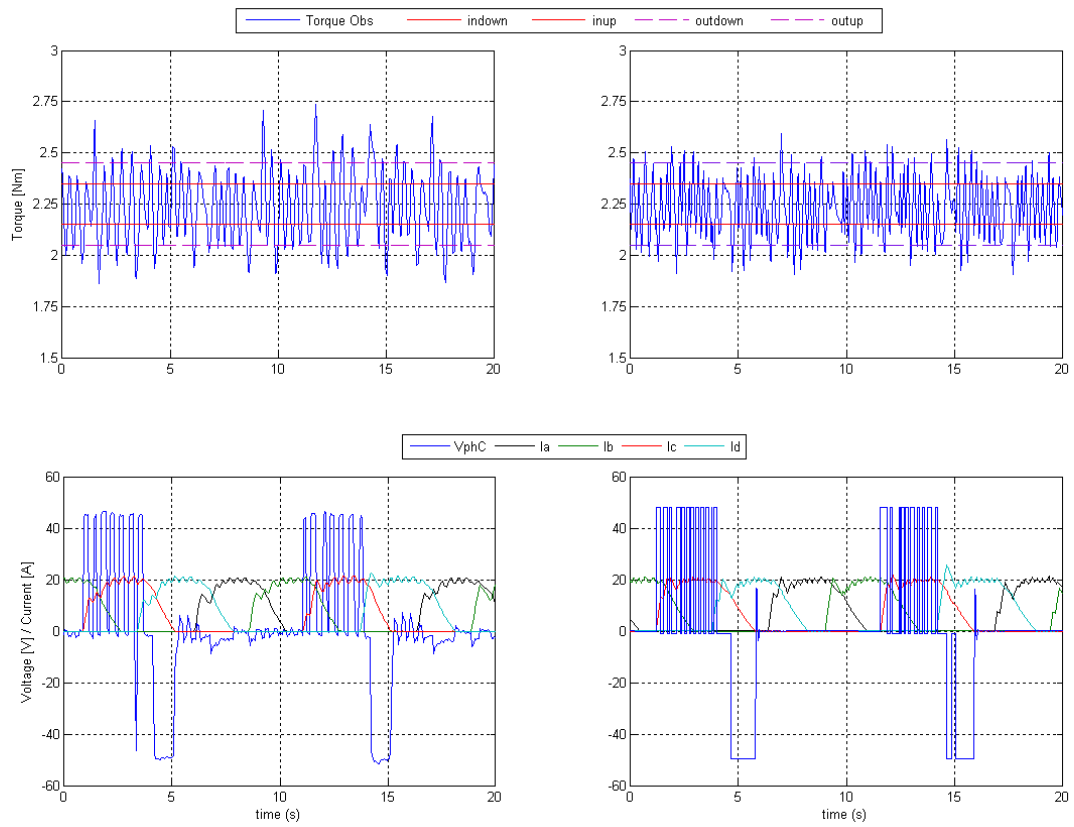


Fig. 10. DITC, experimental waveforms of torque, voltage and current (left) and simulated waveforms (right) ; in both cases, average torque: 2.25 Nm, speed: 960 rpm, $\theta_{ON} = 2^\circ$, $\theta_{OFF} = 22^\circ$.

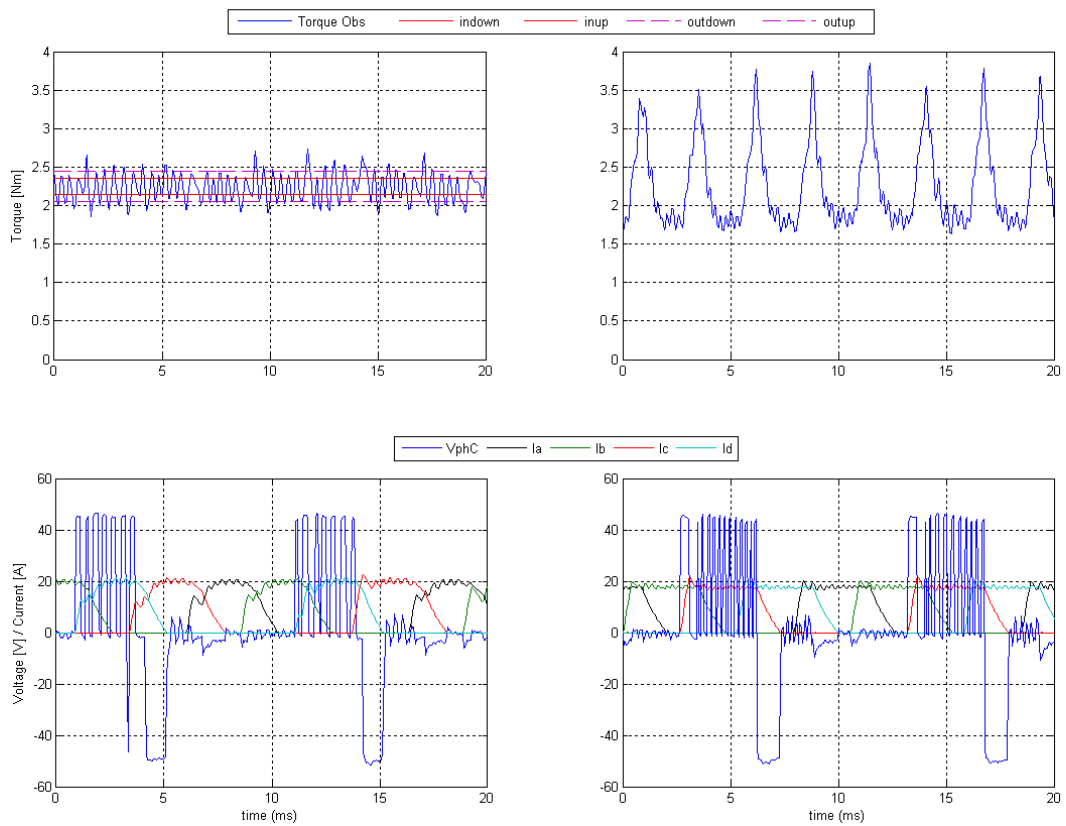


Fig. 11. Experimental waveforms of torque, voltage and current with DITC (left) and experimental waveforms of torque, voltage and current with conventional control (right); in both cases, average torque: 2.25 Nm, speed: 960 rpm, $\theta_{ON} = 2^\circ$, $\theta_{OFF} = 22^\circ$.

3. Simulation model of the DIT controller

A simulation model of the DIT controller is implemented in Matlab/Simulink to verify its successful design. The simulation environment chosen has been Simulink since control models can also be directly implemented in a rapid-prototyping board. Fig 6 shows the DIT controller integration into the real time testing platform including the finite element analysis of the motor. In Fig. 7 the Simulink block diagram of the DIT controller is depicted, according to the structure of Fig 3. The generator of switching logic signals is detailed in Fig 8, which consists of a Mealy machine and a current regulator to avoid high values of current, acting as a motor protection element. The Mealy finite-state machine combines the firing angles with the torque demand provided by the torque hysteresis regulator, and generates the control signals to the power converter switches. The structure of the finite-state machine is represented by a flowchart depicted in Fig. 9. Inside each conduction zone, depending on the result of the decision nodes, the different states are reached (+Vcc/-Vcc/fw). Decision nodes *histin*, *histout(bot)* and *histout(top)* correspond to the torque hysteresis controller signals of inner, outer (bottom) and (top) windows. Simulation will also be useful to contrast the expected and the obtained experimental results.

4. Experimental results

The proposed DITC is implemented in a real time testing platform a DSPACE ACE kit 1006 CLP that included a processor board with an AMD Opteron™ running at 2.6 GHz. The DSPACE ACE kit 1006 CLP is a rapid-prototyping tool that allows controllers to be designed in Simulink, a well-known simulation and prototyping environment for modeling dynamic systems. Once these controllers have been designed, the code is simply generated and loaded into a DSP for real-time control, thus allowing the control algorithm to be tested rapidly. The proposed DITC was tested in a 8/6 SRM prototype, using a set up including the DSPACE ACE kit 1106 and a DC motor acting as a load. In Fig. 10 it can be seen a comparative between experimental and simulated results in both cases for an average torque of 2.25 Nm and an inner and outer hysteresis windows of ± 0.1 and ± 0.2 Nm respectively. A comparative between DITC and a conventional control for the same average torque is shown in Fig. 11.

5. Conclusions

This paper presents some contributions to the minimization of torque ripple in SRM using direct instantaneous torque control (DITC). Direct torque controller is simulated using Matlab/Simulink, previous Finite element analysis of the motor, and then implemented in a DSPACE ACE kit 1006 CLP that includes a processor board with an AMD Opteron™

running at 2.6 GHz. Experimental results are shown and they are compared with those obtained using conventional control demonstrating the goodness of the proposed DITC in SRM drives specially in low speed ranges.

References

- [1] I. Husain, "Minimization of torque ripple in SRM drives", IEEE Transactions on Industrial Electronics, vol. 49, no 1, 2002, pp. 28-39.
- [2] R.B. Inderka, R.W. De Doncker, "DITC – Direct instantaneous torque control of switched reluctance drives", IEEE Transactions on Industry Applications, vol.39, no 4, 2003, pp.1046-1051.
- [3] C.R. Neuhaus, N.H. Fuengwarodsakul, R.W.De Doncker, "Predictive PWM-based direct instantaneous torque control of switched reluctance drives", Power Electronics Specialists Conference, June 2006, pp.1-7
- [4] J. Liang, J. Ahn, D. Lee, "High performance hydraulic pump system using switched reluctance drive", International Conference on Electrical Machines and Systems, October 2007, pp. 1470-1474
- [5] J. Liang, D.H. Lee, J.W. Ahn. "Direct instantaneous torque control of switched reluctance machines using 4-level converters". IET Electr. Power Appl. 2009, Vol.3, Iss. 4, pp. 313-323.
- [6] I. Delgado. "Control de par en un motor SRM aplicado a a dirección asistida en vehículos eléctricos utilizando herramientas de prototipado rápido" (in spanish) Director. B. Blanqué. PFC EPSEVG, 2010.
- [7] F.D'hulster, K.Stockman, R.J.M. Belmans, "Modelling of switched reluctance machines: state of the art", International Journal of Modelling and Simulation, vol. 24, no 4, 2004, pp. 214-223.
- [8] FLUX user's manual, www.cedrat.com

Appendix

Main data of SRM prototype

Stator pole number	8
Rotor pole number	6
Voltage (V)	48
Power (W)	500
Air-gap (mm)	0,35
Rotor air-gap diameter (mm)	56
Stack length (mm)	80
Stator pole angle (°)	22,37°
Rotor pole angle (°)	24,12°
Number of turns per pole	28